Journal of Pathology
J Pathol 2017; **243:** 208–219
Published online 29 August 2017 in Wiley Online Library (wileyonlinelibrary.com) DOI: 10.1002/path.4940

ORIGINAL PAPER

Cytotoxic necrotizing factor 1 promotes prostate cancer progression through activating the Cdc42–PAK1 axis

Yaxiu Guo[1†], Zhisong Zhang[2†], Huiting Wei[1], Jingyu Wang[1], Junqiang Lv[1], Kai Zhang[3,4], Evan T Keller[5], Zhi Yao[1,3*] and Quan Wang[1*]

[1] *Department of Immunology, Key Laboratory of Educational Ministry of China, Tianjin Key Laboratory of Cellular and Molecular Immunology, School of Basic Medical Sciences, Tianjin Medical University, Tianjin, PR China*
[2] *State Key Laboratory of Medicinal Chemical Biology and College of Pharmacy, Collaborative Innovation Center for Biotherapy, and Tianjin Key Laboratory of Molecular Drug Research, Nankai University, Tianjin, PR China*
[3] *2011 Collaborative Innovation Center of Tianjin for Medical Epigenetics, Tianjin Medical University, Tianjin, PR China*
[4] *Tianjin Key Laboratory of Medical Epigenetics, Department of Biochemistry and Molecular Biology, Tianjin Medical University, Tianjin, PR China*
[5] *Department of Urology, University of Michigan, Ann Arbor, Michigan, USA*

**Correspondence to: Quan Wang or Zhi Yao, 22 Qixiangtai Road, Heping District 300070, Tianjin, PR China. E-mail: wangquan@tmu.edu.cn; yaozhi@tmu.edu.cn*

[†]These authors contributed equally to this work.

Abstract

Uropathogenic *Escherichia coli* (UPEC) is the leading cause of urinary tract infections and plays a role in prostatic carcinogenesis and prostate cancer (PCa) progression. However, the mechanisms through which UPEC promotes PCa development and progression are unclear. Cytotoxic necrotizing factor 1 (CNF1) is one of the most important UPEC toxins and its role in PCa progression has never been studied. We found that UPEC-secreted CNF1 promoted the migration and invasion of PCa cells and PCa metastasis. *In vitro* studies showed that CNF1 promotes pro-migratory and pro-invasive activity through entering PCa cells and activating Cdc42, which subsequently induced PAK1 phosphorylation and up-regulation of MMP-9 expression. CNF1 also promoted pulmonary metastasis in a xenograft mouse model through these mechanisms. PAK1 phosphorylation correlated with advanced grades of PCa in human clinical PCa tissues. These results suggest that CNF1 derived from UPEC plays an important role in PCa progression through activating a Cdc42–PAK1 signal axis and up-regulating the expression of MMP-9. Therefore, surveillance for and treatment of *cnf1*-carrying UPEC strains may diminish PCa progression and thus have an important clinical therapeutic impact.

Keywords: cytotoxic necrotizing factor 1; uropathogenic *Escherichia coli*; prostate cancer; Cdc42; PAK1

Received 9 January 2017; Revised 12 June 2017; Accepted 3 July 2017

No conflicts of interest were declared.

Introduction

Uropathogenic *Escherichia coli* (UPEC) is the leading cause of urinary tract infections (UTIs), accounting for most community (~95%) and hospital-acquired (~50%) infections [1]. UTIs caused by UPEC can induce cystitis, pyelonephritis, and prostatitis [2,3]. In addition to being frequently isolated from urine samples of patients with cystitis and pyelonephritis, UPEC is also detected in urine, prostatic secretions, and seminal fluids of patients with prostate cancer (PCa), benign prostatic hyperplasia (BPH), and prostatitis [4,5].

PCa is one of the most common cancers in the western world [6]. In the United States, approximately 2.8 million men are diagnosed with PCa each year, which represents four in ten male cancer survivors and one in five of all cancer survivors [7]. In 2016, it was estimated that there would be 180 890 new PCa cases and 26 120 PCa-related deaths in the United States, resulting in PCa as the most common form of cancer (21%) and ranking as the second most frequent cause of cancer-related death (8%) [8]. Although PCa is not the most common cancer in China, its incidence and mortality rates are rapidly increasing [9]. The 5-year relative survival rate for localized PCa is very high; however, it is low for men with advanced PCa [8].

UPEC infection of male C3H/HeOuJ mice results in prostatic intraepithelial neoplasia (PIN) at 12 weeks, and high-grade prostate dysplasia and invasive PCa 26 weeks after infection [10]. UPEC can accelerate prostatic carcinogenesis induced by 2-amino-1-methyl-6-phenylimidazo[4,5-b]pyridine (PhIP), a dietary carcinogen, and reduces the survival of rats [11]. Pro-oncogenic epithelial changes were found in the prostates of C57BL/6 J mice 8 weeks post-infection

with UPEC [12]. In the genetically engineered Hi-Myc murine PCa model, significantly more UPEC-infected mice had invasive cancer compared with saline-treated mice [12].

Cytotoxic necrotizing factor 1 (CNF1) is a key UPEC toxin. After binding to the surface of epithelial cells, CNF1 is internalized by endocytosis and subsequently transferred to an endosomal compartment, resulting in the enzymatic domain of CNF1 being translocated into the cytoplasm [13,14]. CNF1 induces deamidation of specific glutamine residues of several Rho GTPases including RhoA, Rac1, and Cdc42, resulting in their activation and cell motility [15–18]. The *cnf1* gene can be detected in UPEC strains isolated from patients with prostatitis and in tissue samples of BPH [3,19,20]. The prevalence of *cnf1* in UPEC strains from prostatitis samples is higher than that of samples from cystitis and pyelonephritis [5]. It has also been reported that the prevalence of *E. coli* strains harbouring *cnf1* is higher in biopsies of patients with colorectal cancer than in those of patients with diverticulosis, which implies a role of CNF1 in cancer [21].

In this study, we investigated the role of CNF1 in the motility and invasiveness of PCa cells and PCa metastasis and explored the signalling mechanisms through which CNF1 achieved its activity in PCa progression.

Materials and methods

Cell lines and reagents

The sources of the cell lines and reagents were as follows: PC3, LNCaP, 22Rv1, and VCaP (ATCC, Manassas, VA, USA); the Cdc42 inhibitor CID44216842, RhoA inhibitor CCG-1423, and PAK1 inhibitor IPA3 (SML0918, SML0987 and I2285; Sigma-Aldrich, St Louis, MO, USA); and the Rac1 inhibitor EHT 1864 (HY-16659; MedChem Express, Monmouth Junction, NJ, USA).

Bacterial strains and plasmids

The bacterial strains and plasmids used in this study are listed in the supplementary material, Table S1. All strains were grown at 37 °C in Luria-Bertani (LB) medium for 12 h. When antibiotics were required, they were used at the following final concentrations: kanamycin at 50 μg/ml and ampicillin at 100 μg/ml. The *cnf1* gene from UPEC strains 1 and 11 was amplified by PCR and cloned into pET-28a(+) or pTRC99A. The cDNAs coding for Cdc42 or PAK1 were subcloned into pCMV-Myc or pEGFP-N1. The constructed plasmids and primer sequences are listed in the supplementary material, Tables S1 and S2.

CNF1 recombinant protein expression and purification

CNF1 was purified as previously described [16]. The purified protein was also identified by LC–MS/MS: the corresponding band was excised and subjected to in-gel digestion. The resulting peptides were separated by reverse-phase liquid chromatography on an EASY-nLC 1000 system (Thermo Fisher Scientific, Waltham, MA, USA) and directly sprayed into a Q-Exactive mass spectrometer (Thermo Fisher). All MS/MS spectra were searched against the UniProt-ecoli protein sequence database using the PD search engine (version 2.1.0, Thermo Fisher) with an overall false discovery rate (FDR) for peptides of less than 1%.

Mutagenesis

Mutagenesis of *cnf1*, *CDC42*, and *PAK1* was performed by a round circle polymerase chain reaction-based site-directed Fast Mutagenesis System kit (TransGen Biotech, Beijing, China) according to the manufacturer's protocol. The primers used for mutation were WQ0434 to WQ0437, WQ0465-2 to WQ0468, and WQ0561 to WQ0568 (supplementary material, Table S2).

Wound healing assay

PC3 cells were grown to 95–100% confluency and wounds were generated with a 200 μl pipette tip and treated with buffer, LPS or CNF1 (1 nmol/l). Images of wound healing were taken at the indicated time intervals using a microscope (Leica Microsystems, Wetzlar, Germany). The wound area was measured by ImageJ software.

Transwell migration and invasion assay

Cell migration and invasion assays were performed using Transwell chambers (pore size 8 μm, Costar, Corning 3422), with Corning Matrigel Matrix (Corning Incorporated, Corning, NY, USA) for invasion assays. The inserts were placed in 24-well culture plates. Cells were resuspended in serum-free RPMI 1640 medium. PC3 cells (2×10^5 in 200 μl) were added to the upper chamber of uncoated (for migration assays) or Matrigel-coated (for invasion assays) membranes with CNF1 (1 nmol/l), LPS, or buffer. 600 μl of medium containing 20% fetal bovine serum with CNF1 (1 nmol/l), LPS or buffer was added to the lower chamber as a chemoattractant. After 12 h (migration assays) or 24 h (invasion assays) incubation at 37 °C in a 5% CO_2 humidified atmosphere, the cells that had not migrated through the pores were manually removed from the upper face of the filters using cotton swabs, and cells adherent to the bottom surface of the inserts were fixed in 4% paraformaldehyde for 1 h and stained with 0.1% crystal violet (Beijing Solarbio Science & Technology Co, Ltd, Beijing, China) for 15 min. Finally, the filters were washed three times in PBS and images taken under a microscope (Leica Microsystems) with 200× magnification.

Immunofluorescence analysis

Cells were grown on glass coverslips, fixed with 4% paraformaldehyde for 15 min, and blocked with

phosphate-buffered saline (PBS) containing 10% goat serum for 60 min. Cells were incubated with CNF1 antibody (Santa Cruz Biotechnology, Santa Cruz, CA, USA; sc-52655, 1:200) in PBS at 4 °C overnight, washed three times with PBS, incubated with Alexa Fluor 488-labelled secondary antibody (Life Technologies, Gaithersburg, MD, USA) in PBS for 1 h, and analysed using a confocal fluorescence microscope (FV1000-D; Olympus, Tokyo, Japan).

Rho GTPase activation assays

PC3 cells were seeded in 10 cm dishes. After treatment, Cdc42, Rac1, and RhoA activation was measured using the respective Activation Assay Biochem Kit (Cdc42: BK034; Rac1: BK035; RhoA: BK036, Cytoskeleton, Denver, CO, USA) according to the manufacturer's protocol.

Antibodies and western blotting

Antibodies were obtained from the following companies: anti-phospho-PAK1 (Thr423) (#2601, 1:1000) and anti-PAK1 (#2602, 1:1000) from Cell Signaling Technology, Danvers, MA, USA; anti-MMP2 (sc-10736, 1:500) and anti-CNF1(sc-52655, 1:500) from Santa Cruz Biotechnology; and anti-MMP9 (PB0709, 1:500) from Wuhan Boster Biological Technology Ltd, Wuhan, China. Cells were washed with PBS three times after treatment with CNF1 or dialysis buffer. Whole cell lysates were prepared using RIPA lysis buffer (Millipore, Billerica, MA, USA), adding complete protease inhibitors and phosphatase inhibitors (Roche, Basel, Switzerland). Protein concentration was determined using the BCA Protein Assay Kit (Thermo Fisher) and approximately 40 μg of cell lysates was used. Antibody binding was revealed using an HRP-conjugated anti-rabbit IgG or anti-mouse IgG (Sigma-Aldrich). Antibody complexes were detected using Immobilon Western Chemiluminescent HRP Substrate (Millipore) and exposure to a Tanon-5200 machine. Densitometry was performed using ImageJ software.

Transduction and transfection

PC3 or 22Rv1 cells stably expressing luciferase were constructed using lentiviral supernatant and selected with puromycin following the manufacturer's instructions. PC3-luci cells stably expressing CNF1 or CNF1-C866S (aa 515–1014) were constructed using lentiviral supernatant. PC3 and 22Rv1 cells were transiently transfected with the Cdc42 and PAK1-related plasmids using Lipofectamine 2000 (Invitrogen, Carlsbad, CA, USA).

Tumour xenograft model

Male NOD/SCID mice were purchased from the Academy of Military Medical Science (Beijing, China). All mouse studies were approved by the Animal Ethics Committee of Tianjin Medical University. All animals were 6–8 weeks of age at the time of injection. PC3 cells, expressing luciferase or CNF1 or CNF1-C866S, were resuspended in 300 μl of PBS (Biological Industries) and injected into the lateral tail veins of mice (2×10^6 cells per animal). 22Rv1-luci cells treated with CNF1 or CNF1-C866S (1 nmol/l for 12 h) were resuspended in 50% Matrigel and injected into the prostates of mice (4×10^6 cells per animal).

Mice of both groups were imaged weekly using an IVIS Spectrum scanner (Caliper Life Sciences, Alameda, CA, USA). 200 μl of substrate D-luciferin (Promega, Madison, WI, USA) (3.0 mg) in PBS was injected i.p. in each mouse 10 min prior to imaging. The bioluminescence images were quantified by measuring the total photons over the body and are presented as photons/s per cm^2/sr (sr denotes steradian).

Immunohistochemistry (IHC)

Murine lungs were fixed in 4% paraformaldehyde for 24 h and processed for paraffin embedding. Sections (5 μm) were used for haematoxylin and eosin (H&E) staining and immunohistochemistry for HLA class I (HLA-A, 1:200, 15240-1-AP; Proteintech, Chicago, IL, USA), p-PAK1 (Thr423) (1:10, #2601; Cell Signaling Technology), and MMP-9 (1:100, BA0573; Wuhan Boster).

RNA interference

Double-stranded RNAs as siRNAs for targeted genes and scrambled siRNA (siScr) were synthesized by GenePharma (Shanghai, China). The sequences (sense strand) of the siRNAs are listed in the supplementary material, Table S2. Specific gene knockdowns were assessed by western blotting. Transfection of siRNA was carried out using Lipofectamine 3000 (Invitrogen).

Tissue microarray analysis

The prostate cancer tissue microarray (PR1921a) containing 96 male specimens (8 of normal prostate tissue, 8 of adjacent normal prostate tissues, and 80 malignant tissues with grade II, II–III or III) was purchased from Alenabio (Xi'an, China). Staining was evaluated as described previously [22], and the staining intensity values were determined by Image-Pro Plus software.

Statistical analyses

Data from three independent experiments are presented as the mean ± SD. The statistical significance of differences between groups was calculated using the two-tailed Student's *t*-test or one-way analysis of variance using SPSS 22.0 software.

Phylogenetic analysis

The presence of *cnf1* was found by screening the genome sequences of the 63 UPEC strains used in our previous study [23]. A phylogenetic tree based on the alignments

of combined protein sequences from CNF1 was constructed using maximum likelihood in MEGA 5 with 1000 bootstrap experiments.

Results

CNF1 promotes the migration and invasion of prostate cancer cells *in vitro*

Recombinant CNF1 derived from UPEC strain 11 was purified and validated using mass spectrography (supplementary material, Table S3). PC3 cells were treated with CNF1, LPS or the dialysis buffer as control and then subjected to a wound healing assay. CNF1 induced migration in a dose- and time-dependent manner (Figure 1A, B). Promotion of PC3 migration and invasion by CNF1 were also evaluated in a Transwell assay (Figure 1C, D). We further validated the pro-migratory and pro-invasive effects of CNF1 on other androgen-dependent or -independent PCa cell lines (LNCaP, VCaP, and 22Rv1) (supplementary material, Figure S1A, B). As CNF1 is a typical secretory bacterial protein, we treated PC3 cells with the supernatant from CNF1-overexpressing *E. coli* K12, which increased both the migration and the invasion abilities of PC3 cells (Figure 1E, F).

It has been reported that cysteine 866 and histidine 881 are functional essential amino acid residues of CNF1 [24]. The C866S mutation completely eliminated CNF1's pro-migratory and pro-invasive effects, while H881Q partially blocked activity (Figure 1G, H and supplementary material, Figure S1C). Taken together, these results provide strong evidence that CNF1 has pro-migratory and pro-invasive activity on PCa cells.

CNF1 promotes the *in vivo* metastasis of prostate cancer cells

The effect of CNF1 on the metastasis of PC3 cells was analysed *in vivo* using a xenograft mouse model. PC3 cells were transduced with constitutively expressed luciferase and the CNF1 functional domain (named CNF1c, aa 515–1014, the functional fragment previously reported [14]), or CNF1c-C866S, or a luciferase only control. The expression of luciferase, CNF1c, and CNF1c-C866S was confirmed in the transduced cells. Overexpression of CNF1c protein but not CNF1c-C866S promoted migration and invasion (supplementary material, Figure S2A–C). Control or CNF1c-expressing or CNF1c-C866S-expressing PC3 cells were injected into the tail veins of NOD/SCID mice. Three weeks after injection, mice receiving the PC3 cells with CNF1c overexpression had a higher level of lung metastasis compared with mice receiving the PC3 cells with either CNF1c-C866S or control vector (Figure 2A and supplementary material, Figure S2D). Lung metastasis in mice receiving the CNF1c-overexpressing PC3 cells was identified by H&E staining and by IHC for HLA (Figure 2B, C).

Luciferase-labelled 22Rv1 cells treated with CNF1 or CNF1-C866S were injected into the prostates of NOD/SCID mice. Seven weeks after injection, mice receiving 22Rv1-luci cells treated with CNF1 had a higher level of metastasis (Figure 2D and supplementary material, Figure S2E).

CNF1 activates Rho GTPases in prostate cancer cells

To determine whether CNF1 can enter PCa cells, we treated PC3 cells with CNF1 for 12 h and performed immunofluorescence (IF) for CNF1 protein. There was accumulation of CNF1 protein in the cytoplasm (Figure 3A). We also verified the intracellular presence of CNF1 using western blotting (Figure 3B).

We examined the activation levels of the main three Rho GTPase family members (RhoA, Cdc42, and Rac1) induced by CNF1 using a pull-down assay. RhoA, Cdc42, and Rac1 were activated in PC3 cells treated by CNF1, and among the three GTPases, CNF1's effect was stronger on Cdc42 and Rac1 than on RhoA (Figure 3C–E).

CNF1 promotes the migration and invasion of prostate cancer cells through Cdc42

We hypothesized that CNF1 promoted the motility and invasive properties of PCa cells by activating Rho GTPases, which regulate actin cytoskeletal rearrangement [25]. We blocked the three GTPases using inhibitors (supplementary material, Figure S3A) and found that enhancement of motility and invasion by CNF1 was attenuated in a dose-dependent manner by inhibiting Cdc42, but not Rac1. Inhibition of RhoA reduced PC3 migration and invasion in both the CNF1-treated and the control groups (Figure 4A–F).

Cdc42 expression was knocked down using siRNAs (Figure 4G and supplementary material, Figure S3B). The migration and invasion of Cdc42 knocked-down PC3 cells treated with CNF1 were significantly diminished compared with siScr control (Figure 4H, I). Two other siRNAs targeting different sites of Cdc42 were used to verify our observations (supplementary material, Figure S3C, D). RhoA and Rac1 were also knocked down using siRNA, which did not affect the migration and invasion of PC3 cells promoted by CNF1 (supplementary material, Figure S3E–J).

The activation level of Cdc42 in the androgen-dependent cell line 22Rv1 was also upregulated after treatment of CNF1 (supplementary material, Figure S3 K). To determine the role of active Cdc42 in the migration and invasion of PCa cells, Cdc42 or constitutively active Cdc42 (CA-Cdc42, Q61E; Q61 was reported to be deamidated by CNF1 [17]) or dominant negative Cdc42 (DN-Cdc42, T17 N) was transfected into PC3 (androgen-independent) or 22Rv1 (androgen-dependent) cells. PCa cells transfected with CA-Cdc42 had higher levels of active Cdc42 and their migration and invasion abilities were significantly increased compared with PCa cells transfected with

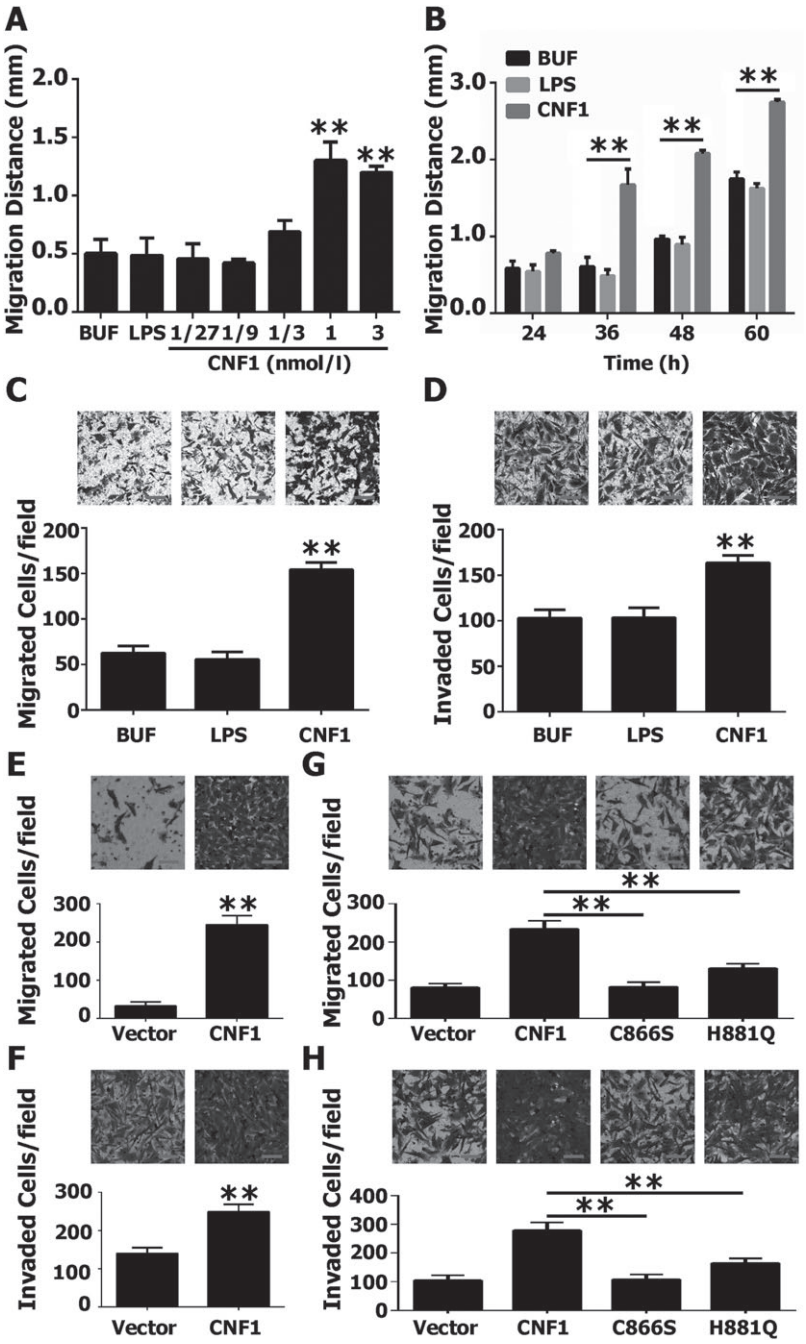

Figure 1. CNF1 promotes the migration and invasion ability of PCa cells. (A) Migration ability in the wound healing assay of PC3 cells treated with recombinant CNF1 protein in different doses, dialysis buffer, and LPS as the control. (B) Time-dependent migration assay of CNF1 (1 nmol/l) on PC3 cells. (C, D) Transwell-based migration and invasion assays of PC3 cells treated with 1 nmol/l CNF1. (E, F) Migration and invasion assays of PC3 cells treated with supernatant from overexpressed CNF1 or vector in *E. coli* K12. (G, H) Migration and invasion assays of PC3 cells treated with supernatant from different strains overexpressing wild-type CNF1 and CNF1 mutant C866S or H881Q (blank vector as the negative control). Bar graphs represent data from three independent assays (mean ± SD). $^{**}p < 0.01$; one-way ANOVA (A–D, G, and H) or Student's *t*-test (E, F). Scale bar = 50 μm.

Cdc42 or DN-Cdc42 (Figure 4J–L and supplementary material, Figure S4A–C).

Cdc42-mediated phosphorylation of PAK1 is essential for the enhancement of prostate cancer cell migration and invasion induced by CNF1

Group I p21-activated kinase 1 (PAK1) is an important effector of the small GTPase Cdc42 [26] and acts as an important regulator of cytoskeletal dynamics and cell motility [27]. To determine the pro-migratory and pro-invasive effects of CNF1 on PC3 cells, we blocked this pathway with the PAK1 inhibitor (IPA3) [28]. Exposure of CNF1-treated PC3 cells to IPA3 decreased their migration and invasion in a dose-dependent manner (Figure 5A, B), indicating that CNF1 promotes these activities through PAK1. Thr423 phosphorylation is required for full activation of PAK1 [28] and we found

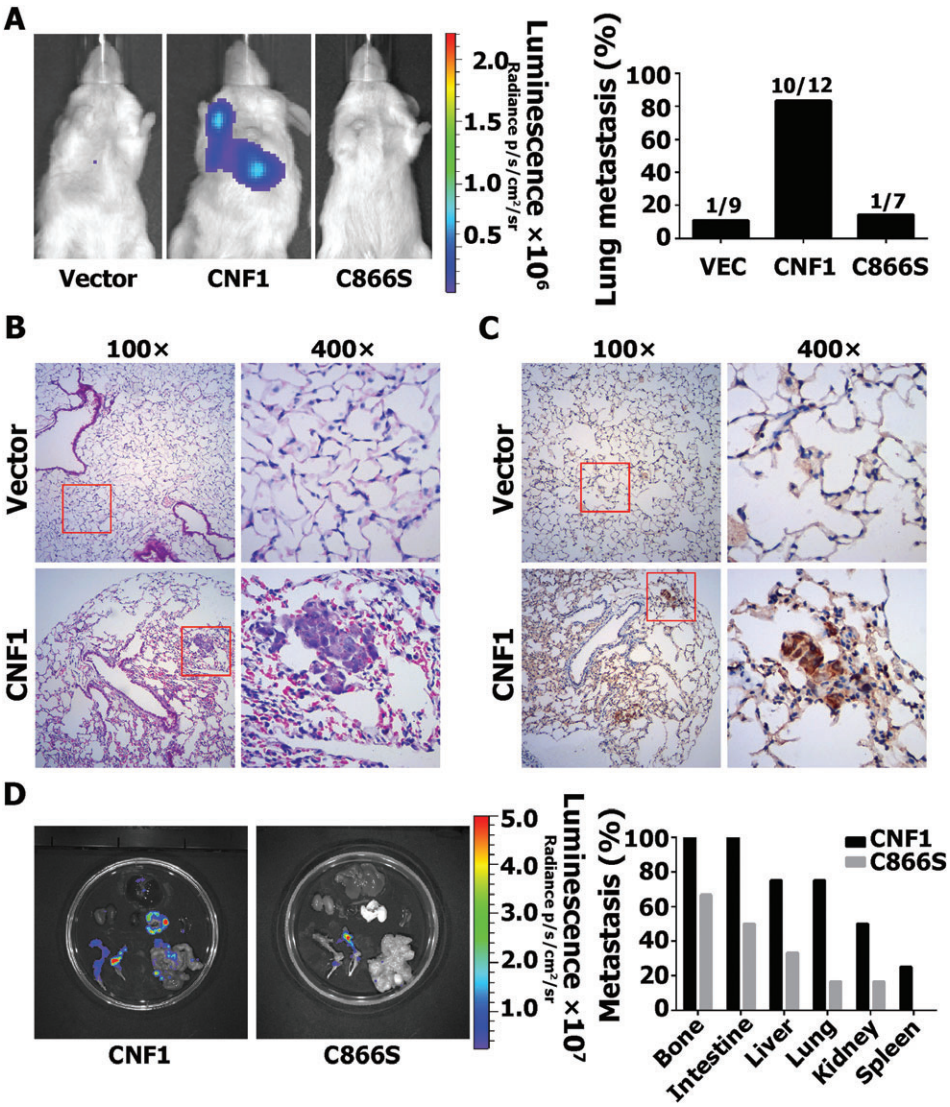

Figure 2. CNF1 promotes the *in vivo* metastasis of prostate cancer cells in a xenograft mouse model. (A) Luciferase-labelled PC3 cells without CNF1 expression ($N = 9$), with CNF1 expression ($N = 12$) or with CNF1-C866S expression ($N = 7$) (2×10^6) were injected into NOD/SCID mice via the lateral tail vein, and bioluminescence imaging of live mice was performed at the third week. (B) H&E staining of lung tissue showing significant metastasis in the CNF1 group (original magnification 100× and 400×) and normal tissue in the control group. (C) Immunohistochemical analysis of murine lung with PC3 cells staining HLA-A with a specific antibody (original magnification 100× and 400×). (D) Luciferase-labelled 22Rv1 cells treated with CNF1 ($N = 4$) or CNF1-C866S ($N = 6$) (4×10^6) were injected into the prostates of NOD/SCID mice, and bioluminescence imaging of live mice was performed at the seventh week.

elevated phosphorylation of PAK1 at Thr423 after treatment with CNF1 (Figure 5C). Elevated phosphorylation of PAK1 was also identified in 22Rv1 cells treated with CNF1 (Figure 5D).

To determine the role of PAK1 phosphorylation in the migration and invasion of PCa cells, PAK1 or constitutively active PAK1 (CA-PAK1, T423E) or dominant negative PAK1 (DN-PAK1, K299R) was transfected into PC3 and 22Rv1 cells. The migration and invasion abilities of PCa cells transfected with CA-PAK1 were significantly increased compared with PCa cells transfected with PAK1 or DN-PAK1 (Figure 5E–G and supplementary material, Figure S5A–C).

As we identified that CNF1 mediates its activity, in part, through Cdc42, we next investigated whether PAK1 activation is directly mediated by Cdc42 activation. The Cdc42 inhibitor CID44216842 inhibited phosphorylation of PAK1 (Figure 5H), and increased PAK1 phosphorylation was found in PC3 and 22Rv1 cells transfected with CA-Cdc42 compared with those transfected with Cdc42 or DN-Cdc42 (Figure 4J and supplementary material, Figure S4A). These findings demonstrate that CNF1 activates Cdc42–PAK1 signalling to promote the migration and invasion of prostate cancer cells.

CNF1 up-regulates the expression of MMP-9 by activating PAK1

Nearly every member of the matrix metalloproteinase (MMP) family has been reported to be dysregulated in human cancers, with the gelatinases (MMP-2 and

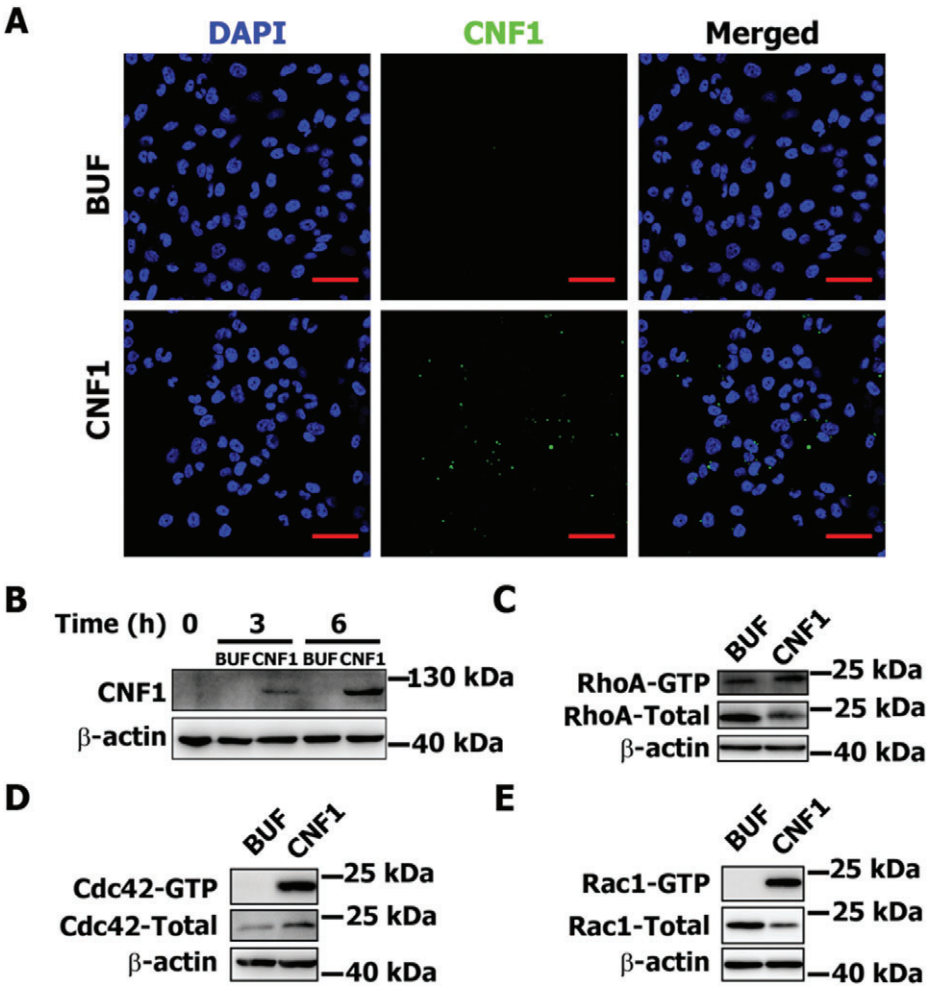

Figure 3. CNF1 activates Rho GTPases in PCa cells. (A) Representative immunofluorescence images of PC3 cells treated with recombinant CNF1 protein (1 nmol/l) for 12 h. Blue, nucleus; green, CNF1. Scale bar = 50 μm. (B) Western blotting analysis of CNF1 protein in PC3 cells cultured with CNF1 recombinant protein (1 nmol/l) for 3 and 6 h. β-Actin was the loading control. (C–E) Western blotting analysis of activated Rho GTPases. RhoA, Cdc42, and Rac1 in PC3 cells [treated with recombinant CNF1 protein (1 nmol/l) or dialysis buffer for 12 h] after immunoprecipitation with GTP pull-down assays using specific antibodies.

MMP-9) playing a pivotal role in degrading the extracellular matrix (ECM) [29]. We explored whether the pro-invasive effect is associated with MMP-9 or MMP-2. CNF1 up-regulated MMP-9, but had no effect on MMP-2 expression. PAK1 inhibition diminished the ability of CNF1 to up-regulate MMP-9 (Figure 6A). Increased MMP-9 was found in PC3 and 22Rv1 cells transfected with CA-PAK1 compared with PCa cells transfected with PAK1 or DN-PAK1 (Figure 5E and supplementary material, Figure S5A). These results demonstrate that CNF1 can up-regulate the expression of MMP-9 by activating PAK1. Inhibition of Cdc42 also significantly reduced the expression of MMP-9, but not of MMP-2 (Figure 6B). The level of active Cdc42, PAK1 phosphorylation, and MMP-9 expression were also up-regulated in PC3 cells with CNF1c overexpression compared with those with CNF1c-C866S or the control vector (supplementary material, Figure S2F). These results demonstrate that CNF1 can drive the migration and invasion of PCa cells through the Cdc42–PAK1–MMP-9 pathway *in vitro*.

To further validate the role for CNF1 in promoting PCa invasion through PAK1 and MMP-9, we performed IHC analysis of lung tissue from the experimental mice described previously. MMP-9 and phosphorylated PAK1 expression were present in the pulmonary metastases of mice injected by PC3 cells with CNF1c expression (Figure 6C). These results suggest a key role for the Cdc42–PAK1–MMP-9 signalling axis in CNF1-induced PCa aggressiveness *in vivo*.

Activation of PAK1 is positively correlated with advanced human prostate cancer

The expression of phosphorylated PAK1 was analysed by IHC using a human tissue array containing 96 samples, which included 80 PCa tissues of grade II, II–III, or III. The percentage of samples with phosphorylated PAK1 staining in malignant tissues was higher than those in normal and adjacent normal tissues and was positively correlated with the histological grade of the PCa (Figure 6D, E). We also found that the levels of phosphorylated PAK1 were strongly correlated with PCa grade

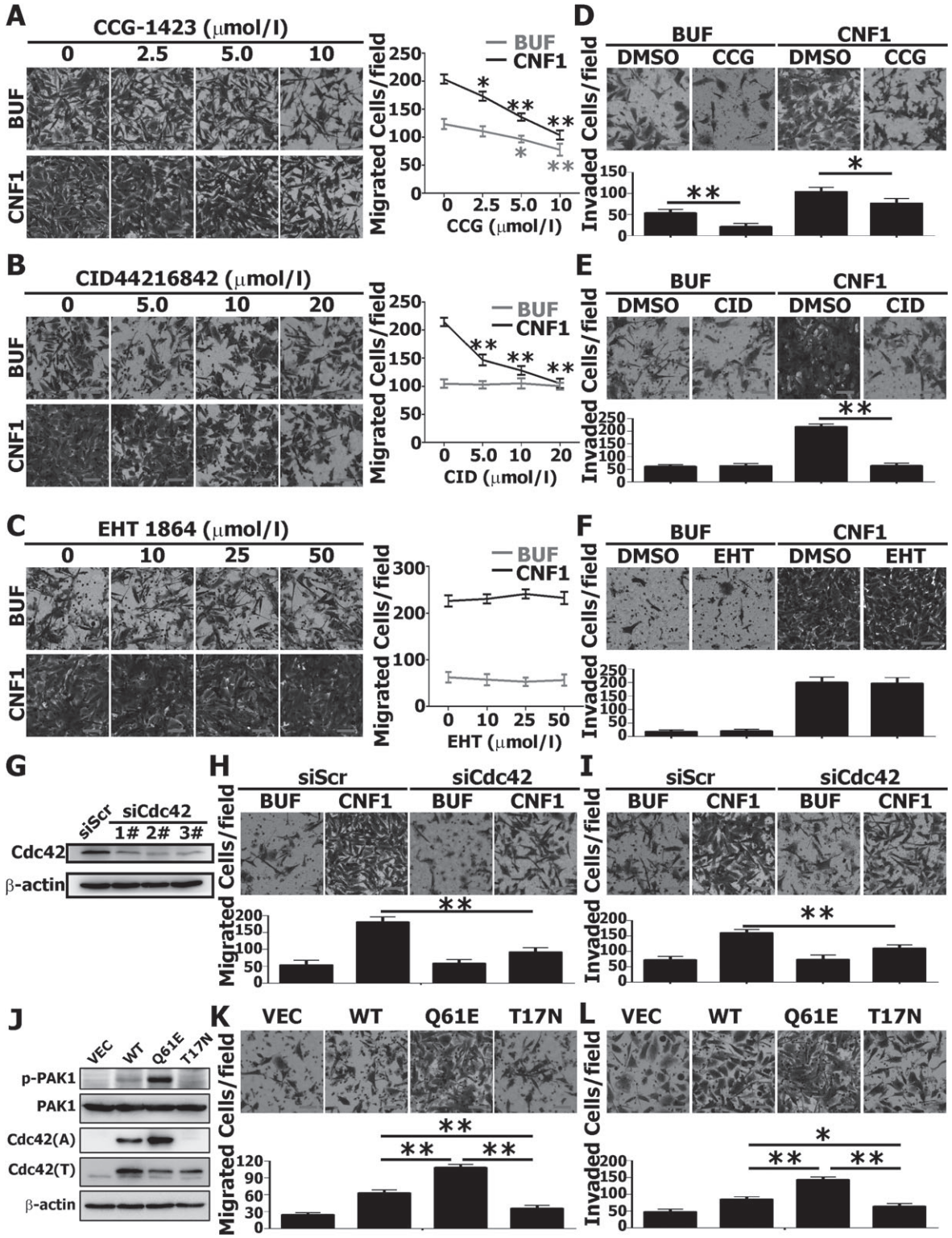

Figure 4. CNF1 promotes the migration and invasion of PCa cells through Cdc42. (A–C) Transwell migration assays of PC3 cells treated with specific inhibitors of RhoA (CCG-1423), Cdc42 (CID44216842), and Rac1 (EHT 1864) in different concentrations and 1 nmol/l CNF1 (or dialysis buffer). Line graphs represent data from three independent assays. (D–F) Invasion assays of PC3 cells treated with specific inhibitors for Rho GTPases with CNF1 protein. (G) Western blotting analysis of PC3 cells treated with siRNAs targeting Cdc42 and scrambled non-targeting control siRNA. (H, I) Migration and invasion assays of CNF1-treated PC3 cells after being transfected with Cdc42 or scramble siRNAs. (J) Western blotting analysis of PC3 cells transfected with vector, Cdc42, constitutively active Cdc42 or dominant negative Cdc42. (K, L) Migration and invasion assays of PC3 cells transfected with vector, Cdc42, constitutively active Cdc42 or dominant negative Cdc42. Bar graphs represent data from three independent assays (mean ± SD). *$p < 0.05$; **$p < 0.01$; one-way ANOVA (A–F, H, I, K, and L). Scale bar = 50 μm.

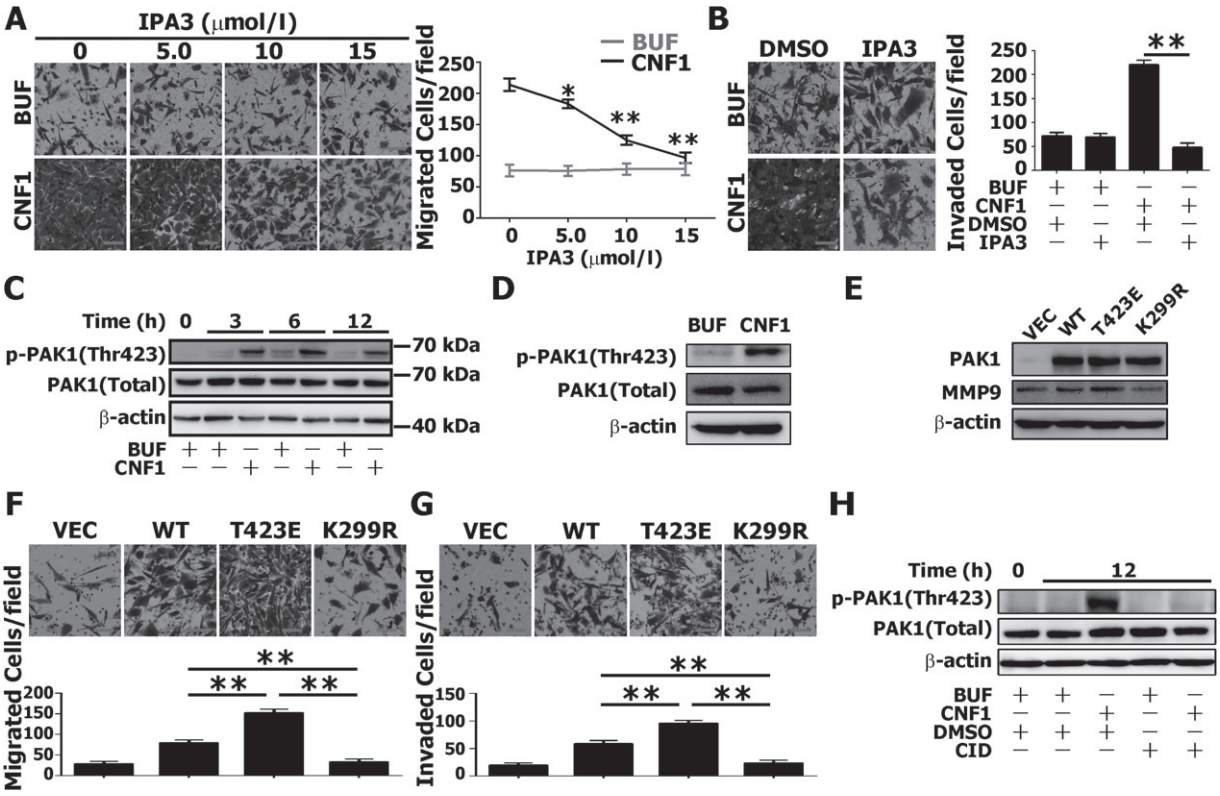

Figure 5. Cdc42-mediated phosphorylation of PAK1 is essential for the enhancement of PCa cell migration and invasion by CNF1. (A) Migration assays of PC3 cells cultured with the PAK1 inhibitor IPA3 in different concentrations accompanied with CNF1 protein or dialysis buffer. The line graph represents data from three independent experiments. (B) Invasion assays of PC3 cells under the treatment of IPA3 and CNF1, DMSO, and dialysis buffer as the specific control. The bar graph represents data from three independent assays. (C) Western blotting analysis of activated PAK1 (phosphorylated on Thr423) and total PAK1 in PC3 cells after treatment with CNF1 protein (1 nmol/l) at 3–12 h. (D) Western blotting analysis of 22Rv1 cells treated with CNF1 or dialysis buffer. (E) Western blotting analysis of PC3 cells transfected with vector, PAK1, constitutively active PAK1 or dominant negative PAK1. (F, G) Migration and invasion assays of PC3 cells transfected with vector, PAK1, constitutively active PAK1 or dominant negative PAK1. (H) Analysis of activated PAK1 and total PAK1 of PC3 cells under treatment of the Cdc42 inhibitor CID44216842 and CNF1 protein, with DMSO and dialysis buffer as the control. Bar graphs represent data from three independent assays (mean ± SD). *$p < 0.05$; **$p < 0.01$; one-way ANOVA (A, B, F, G). Scale bar = 50 μm.

(Figure 6F), and the positive percentage of samples with strong staining was higher in grades III and II–III than in grade II tissues (Figure 6G). These results indicate that PAK1 activation is correlated with PCa advanced grades.

CNF1 derived from other UPECs has similar pro-migratory and pro-invasive effects on prostate cancer cells

We found that 11 of 63 UPEC strains with available genome sequences included the *cnf1* gene. The 11 CNF1 proteins were separated into two groups, with two different amino acids (N666T, V1001A) in the segment of 515–1014 (supplementary material, Figure S6A). We purified another recombinant CNF1 derived from UPEC strain 1, which belongs to a different UPEC group than UPEC strain 11. Consistent with the results obtained from the UPEC strain 11-derived CNF1, UPEC strain 1-derived CNF1 also promoted the migration and invasion of PC3 cells (supplementary material, Figure S6B, C). Additionally, we detected the effects of Cdc42, Rac1, RhoA, and PAK1 inhibitors on strain 1-derived CNF1-induced cell migration and invasion (supplementary material, Figure S6D, E). The changes of MMP-9 expression and PAK1 phosphorylation level induced by CNF1 (strain 1) were also examined using western blotting (supplementary material, Figure S6F).

Three UPEC strain 11-derived CNF1 mutants – N666T, V1001A, and double mutant – were created. Wild-type and mutant CNF1-overexpressed *E. coli* K12 were used to perform phenotype experiments, and no obvious difference was observed on PC3 cell migration and invasion (supplementary material, Figure S6G–I). These findings demonstrate that CNF1 derived from other UPECs has similar pro-migratory and pro-invasive effects on prostate cancer cells and that residues 666 and 1001 do not influence CNF1 activity.

Discussion

In this study, we identified that CNF1 secreted by UPEC could accelerate PCa progression through activating the Cdc42–PAK1 signalling axis (supplementary material, Figure S7). Almost 20% of all cancers are associated with microbial infection [30], and certain cancer types are promoted by bacteria. *Helicobacter pylori* is a prime example that bacterial pathogens can drive

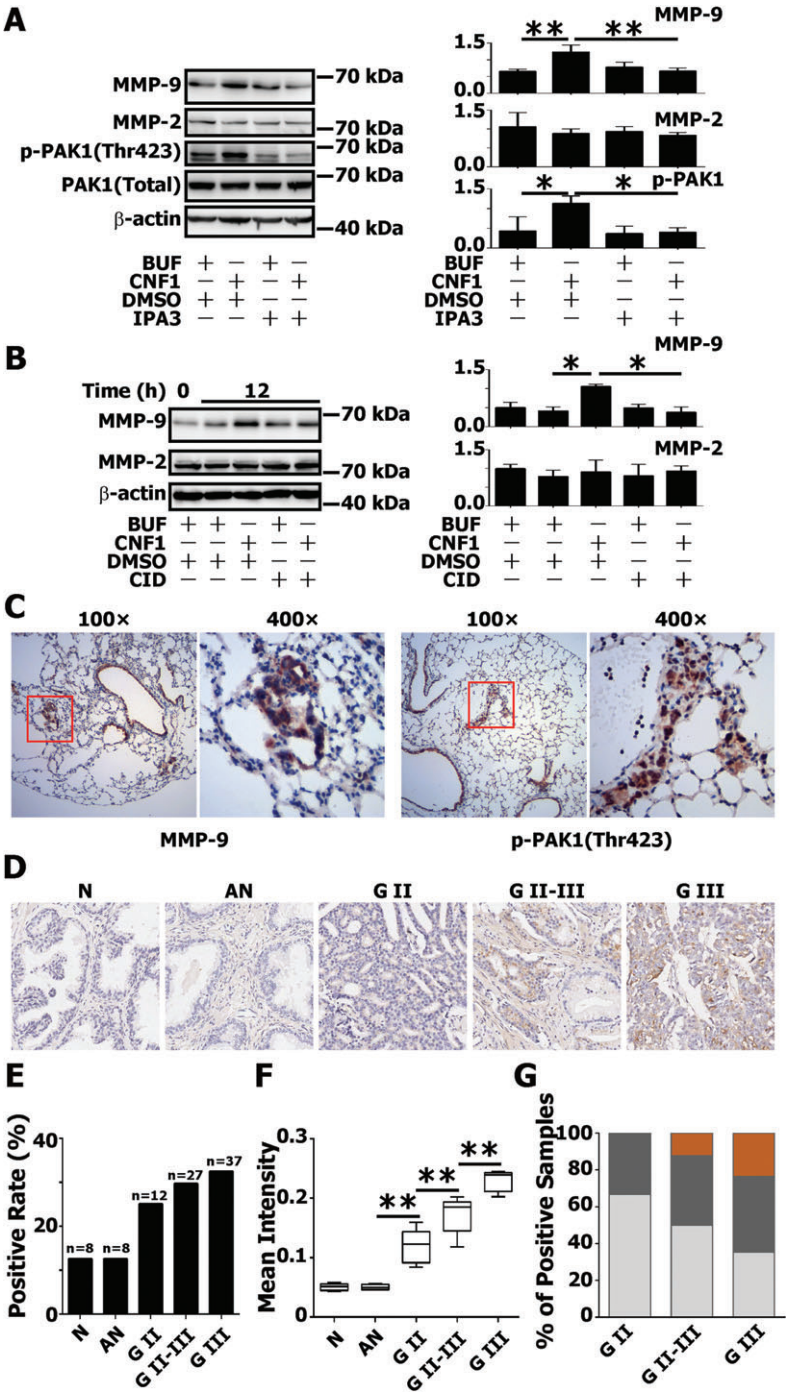

Figure 6. CNF1 up-regulates the expression of MMP9 through the Cdc42–PAK1 axis and active PAK1 is positively correlated with advanced-grade PCa. (A, B) Western blotting analysis of metastasis-associated metalloproteinases MMP-9 and MMP-2 in PC3 cells treated with the PAK1 inhibitor IPA3 or the Cdc42 inhibitor CID44216842 with CNF1 protein or dialysis buffer. (C) IHC of murine lung specimens from the CNF1-overexpressed PC3 xenograft metastasis model for MMP-9 and activated PAK1 (original magnification 100× and 400×). (D) IHC analysis of PAK1 phosphorylation using human PCa tissue microarray. Representative images (original magnification 200×) from normal prostate tissues, adjacent normal prostate tissues, and malignant prostate tissues with grade II, II–III or III are shown. (E) Percentage of samples with positively stained p-PAK1. *n* indicates the sample size in different groups. (F) Mean intensity of staining determined by Image-Pro Plus software and presented with box plots. (G) Percentage of samples with high (orange), medium (dark grey), and weak (light grey) staining of p-PAK1 in positively stained samples with different grades. Data are mean ± SD. $^{*}p < 0.05$; $^{**}p < 0.01$; one-way ANOVA (A, B, F).

carcinogenesis and has been classified as a carcinogen for gastric cancer by the International Agency for Research on Cancer (IARC) [31,32]. Other pathogenic bacteria such as *Salmonella enterica*, *Borrelia burgdorferi*, *Chlamydia psittaci*, and *Staphylococcus aureus* have been reported to be associated with gallbladder cancer and certain kinds of lymphomas [33–37]. A few bacterial virulence factors have been identified to promote cancer by interacting with human signalling pathways, such as CagA and VacA of *H. pylori* and SEA

of *S. aureus* [36,38]. The possible roles for many other bacterial toxins on cancer development and progression remain to be clarified.

Cdc42 expression is up-regulated in many kinds of cancers such as breast, colorectal, and ovarian cancer [39,40]. The role of Cdc42 in prostate cancer is rarely reported. The p21-activated kinases (PAKs) are overexpressed and activated in many human cancers and are positively correlated with advanced grades and decreased survival; PAK1 is one of the best characterized PAKs dysregulated in cancers [41]. PAK1 up-regulates MMP expression in breast cancer cells [42]. Higher expression of PAK1 was found in invasive PCa cells compared with non-invasive PCa cells, and inhibition of PAK1 impaired PC3 cell migration [43]. It was suggested that this effect was caused by high expression of MMP-9 and low expression of TGFβ regulated by PAK1 [43]. In our study, CNF1 increased the phosphorylation of PAK1 by activating Cdc42 and then up-regulated the expression of MMP-9. Up-regulation of active PAK1 correlated with advanced-grade PCa using clinical human PCa samples, indicating that active PAK1 is a possible marker, although further experiments are required.

Only UPEC strains CP1 and CP9 have been used to infect the prostate in mouse or rat models in previous reports [11,12,44]. In our study, UPEC strains 1 and 11 could not successfully infect the prostates of NOD/SCID mice and C57BL/6 J mice, indicating that UPEC strains used for prostate infection in mouse models are very limited. CNF1 has been reported to enhance inflammation in bladder and prostate [44,45], and we also found that bladder inflammation caused by the CNF1-overexpressing K12 strain was greater than that caused by the CNF1-C866S-overexpressing K12 stain and the K12 control strain (data not shown). Therefore, in addition to the migratory and invasive activity of PCa cells promoted by CNF1, CNF1-inducing inflammation may also promote PCa progression, which needs further studies.

Acknowledgements

This study was supported by grants from the National Natural Science Foundation of China (NSFC) Programs (31670071, 81672740, and 31270016) and the State Key Laboratory of Medicinal Chemical Biology (201601009). We thank Dr Antoni Rozalski and Agata Palusiak from the University of Lodz for supplying UPEC strains, and members of Dr Wang's and Dr Yao's laboratory for helpful technical assistance.

Author contributions statement

QW designed the study. YG, JW, ZZ, and KZ performed the majority of the experiments. HW and JL performed parts of the cell and animal experiments. QW, YG, ZZ, and ZY analysed the data and wrote the paper. Experimental design assistance and manuscript revision were provided by EK. All authors discussed the data and reviewed and approved the manuscript.

References

1. Jacobsen SM, Stickler DJ, Mobley HL, *et al.* Complicated catheter-associated urinary tract infections due to *Escherichia coli* and *Proteus mirabilis*. *Clin Microbiol Rev* 2008; **21:** 26–59.
2. Nielubowicz GR, Mobley HL. Host–pathogen interactions in urinary tract infection. *Nat Rev Urol* 2010; **7:** 430–441.
3. Mitsumori K, Terai A, Yamamoto S, *et al.* Virulence characteristics of *Escherichia coli* in acute bacterial prostatitis. *J Infect Dis* 1999; **180:** 1378–1381.
4. Yu H, Meng H, Zhou F, *et al.* Urinary microbiota in patients with prostate cancer and benign prostatic hyperplasia. *Arch Med Sci* 2015; **11:** 385–394.
5. Johnson JR, Kuskowski MA, Gajewski A, *et al.* Extended virulence genotypes and phylogenetic background of *Escherichia coli* isolates from patients with cystitis, pyelonephritis, or prostatitis. *J Infect Dis* 2005; **191:** 46–50.
6. Crawford ED. Understanding the epidemiology, natural history, and key pathways involved in prostate cancer. *Urology* 2009; **73:** S4–S10.
7. Skolarus TA, Wolf AM, Erb NL, *et al.* American Cancer Society prostate cancer survivorship care guidelines. *CA Cancer J Clin* 2014; **64:** 225–249.
8. Siegel RL, Miller KD, Jemal A. Cancer statistics, 2016. *CA Cancer J Clin* 2016; **66:** 7–30.
9. Chen W, Zheng R, Baade PD, *et al.* Cancer statistics in China, 2015. *CA Cancer J Clin* 2016; **66:** 115–132.
10. Elkahwaji JE, Hauke RJ, Brawner CM. Chronic bacterial inflammation induces prostatic intraepithelial neoplasia in mouse prostate. *Br J Cancer* 2009; **101:** 1740–1748.
11. Sfanos KS, Canene-Adams K, Hempel H, *et al.* Bacterial prostatitis enhances 2-amino-1-methyl-6-phenylimidazo[4,5-b]pyridine (PhIP)-induced cancer at multiple sites. *Cancer Prev Res* 2015; **8:** 683–692.
12. Simons BW, Durham NM, Bruno TC, *et al.* A human prostatic bacterial isolate alters the prostatic microenvironment and accelerates prostate cancer progression. *J Pathol* 2015; **235:** 478–489.
13. Kim KJ, Chung JW, Kim KS. 67-kDa laminin receptor promotes internalization of cytotoxic necrotizing factor 1-expressing *Escherichia coli* K1 into human brain microvascular endothelial cells. *J Biol Chem* 2005; **280:** 1360–1368.
14. Knust Z, Blumenthal B, Aktories K, *et al.* Cleavage of *Escherichia coli* cytotoxic necrotizing factor 1 is required for full biologic activity. *Infect Immun* 2009; **77:** 1835–1841.
15. Schmidt G, Sehr P, Wilm M, *et al.* Gln 63 of Rho is deamidated by *Escherichia coli* cytotoxic necrotizing factor-1. *Nature* 1997; **387:** 725–729.
16. Flatau G, Lemichez E, Gauthier M, *et al.* Toxin-induced activation of the G protein p21 Rho by deamidation of glutamine. *Nature* 1997; **387:** 729–733.
17. Lerm M, Selzer J, Hoffmeyer A, *et al.* Deamidation of Cdc42 and Rac by *Escherichia coli* cytotoxic necrotizing factor 1: activation of c-Jun N-terminal kinase in HeLa cells. *Infect Immun* 1999; **67:** 496–503.
18. Doye A, Mettouchi A, Bossis G, *et al.* CNF1 exploits the ubiquitin-proteasome machinery to restrict Rho GTPase activation for bacterial host cell invasion. *Cell* 2002; **111:** 553–564.
19. Andreu A, Stapleton AE, Fennell C, *et al.* Urovirulence determinants in *Escherichia coli* strains causing prostatitis. *J Infect Dis* 1997; **176:** 464–469.

20. Bergh J, Marklund I, Thellenberg-Karlsson C, *et al.* Detection of *Escherichia coli* 16S RNA and cytotoxic necrotizing factor 1 gene in benign prostate hyperplasia. *Eur Urol* 2007; **51:** 457–462.
21. Buc E, Dubois D, Sauvanet P, *et al.* High prevalence of mucosa-associated *E. coli* producing cyclomodulin and genotoxin in colon cancer. *PLoS One* 2013; **8:** e56964.
22. Reiner A, Neumeister B, Spona J, *et al.* Immunocytochemical localization of estrogen and progesterone receptor and prognosis in human primary breast cancer. *Cancer Res* 1990; **50:** 7057–7061.
23. Ren Y, Palusiak A, Wang W, *et al.* A high-resolution typing assay for uropathogenic *Escherichia coli* based on fimbrial diversity. *Front Microbiol* 2016; **7:** 623.
24. Schmidt G, Selzer J, Lerm M, *et al.* The Rho-deamidating cytotoxic necrotizing factor 1 from *Escherichia coli* possesses transglutaminase activity. Cysteine 866 and histidine 881 are essential for enzyme activity. *J Biol Chem* 1998; **273:** 13669–13674.
25. van Buul JD, Timmerman I. Small Rho GTPase-mediated actin dynamics at endothelial adherens junctions. *Small GTPases* 2016; **7:** 21–31.
26. Ye DZ, Field J. PAK signaling in cancer. *Cell Logist* 2012; **2:** 105–116.
27. Bokoch GM. Biology of the p21-activated kinases. *Annu Rev Biochem* 2003; **72:** 743–781.
28. Deacon SW, Beeser A, Fukui JA, *et al.* An isoform-selective, small-molecule inhibitor targets the autoregulatory mechanism of p21-activated kinase. *Chem Biol* 2008; **15:** 322–331.
29. Cathcart J, Pulkoski-Gross A, Cao J. Targeting matrix metalloproteinases in cancer: bringing new life to old ideas. *Genes Dis* 2015; **2:** 26–34.
30. Elinav E, Nowarski R, Thaiss CA, *et al.* Inflammation-induced cancer: crosstalk between tumours, immune cells and microorganisms. *Nat Rev Cancer* 2013; **13:** 759–771.
31. Peek RM Jr, Blaser MJ. *Helicobacter pylori* and gastrointestinal tract adenocarcinomas. *Nat Rev Cancer* 2002; **2:** 28–37.
32. Fox JG, Wang TC. Inflammation, atrophy, and gastric cancer. *J Clin Invest* 2007; **117:** 60–69.
33. Caygill CP, Hill MJ, Braddick M, *et al.* Cancer mortality in chronic typhoid and paratyphoid carriers. *Lancet* 1994; **343:** 83–84.
34. Senff NJ, Noordijk EM, Kim YH, *et al.* European Organization for Research and Treatment of Cancer and International Society for Cutaneous Lymphoma consensus recommendations for the management of cutaneous B-cell lymphomas. *Blood* 2008; **112:** 1600–1609.
35. Ferreri AJ, Govi S, Pasini E, *et al. Chlamydophila psittaci* eradication with doxycycline as first-line targeted therapy for ocular adnexae lymphoma: final results of an international phase II trial. *J Clin Oncol* 2012; **30:** 2988–2994.
36. Willerslev-Olsen A, Krejsgaard T, Lindahl LM, *et al. Staphylococcus aureus* enterotoxin A (SEA) stimulates STAT3 activation and IL-17 expression in cutaneous T-cell lymphoma. *Blood* 2016; **127:** 1287–1296.
37. Krejsgaard T, Willerslev-Olsen A, Lindahl LM, *et al.* Staphylococcal enterotoxins stimulate lymphoma-associated immune dysregulation. *Blood* 2014; **124:** 761–770.
38. Ohnishi N, Yuasa H, Tanaka S, *et al.* Transgenic expression of *Helicobacter pylori* CagA induces gastrointestinal and hematopoietic neoplasms in mouse. *Proc Natl Acad Sci U S A* 2008; **105:** 1003–1008.
39. Bray K, Gillette M, Young J, *et al.* Cdc42 overexpression induces hyperbranching in the developing mammary gland by enhancing cell migration. *Br J Cancer* 2013; **15:** R91.
40. Sakamori R, Yu S, Zhang X, *et al.* CDC42 inhibition suppresses progression of incipient intestinal tumors. *Cancer Res* 2014; **74:** 5480–5492.
41. Radu M, Semenova G, Kosoff R, *et al.* PAK signalling during the development and progression of cancer. *Nat Rev Cancer* 2014; **14:** 13–25.
42. Rider L, Oladimeji P, Diakonova M. PAK1 regulates breast cancer cell invasion through secretion of matrix metalloproteinases in response to prolactin and three-dimensional collagen IV. *Mol Endocrinol* 2013; **27:** 1048–1064.
43. Goc A, Al-Azayzih A, Abdalla M, *et al.* P21 activated kinase-1 (Pak1) promotes prostate tumor growth and microinvasion via inhibition of transforming growth factor beta expression and enhanced matrix metalloproteinase 9 secretion. *J Biol Chem* 2013; **288:** 3025–3035.
44. Rippere-Lampe KE, Lang M, Ceri H, *et al.* Cytotoxic necrotizing factor type 1-positive *Escherichia coli* causes increased inflammation and tissue damage to the prostate in a rat prostatitis model. *Infect Immun* 2001; **69:** 6515–6519.
45. Garcia TA, Ventura CL, Smith MA, *et al.* Cytotoxic necrotizing factor 1 and hemolysin from uropathogenic *Escherichia coli* elicit different host responses in the murine bladder. *Infect Immun* 2013; **81:** 99–109.

SUPPLEMENTARY MATERIAL ONLINE

Supplementary figure legends

Figure S1. CNF1 promotes the migration and invasion ability of PCa cell lines LNCaP, 22Rv1, and VCaP

Figure S2. CNF1 promotes PCa progression *in vivo*

Figure S3. Knockdown of Cdc42 diminished the migration and invasion of PC3 cells

Figure S4. Overexpression of active Cdc42 promoted the migration and invasion of 22Rv1 cells

Figure S5. Overexpression of active PAK1 promoted the migration and invasion of 22Rv1 cells

Figure S6. CNF1 derived from other UPECs has similar pro-migratory and pro-invasive effects on PCa cells

Figure S7. A model of CNF1 promoting PCa cell migration and invasion

Table S1. Strains and plasmids used in this study

Table S2. Primers and siRNAs used in this study

Table S3. Peptides identified for CNF1